## Supplementary materials

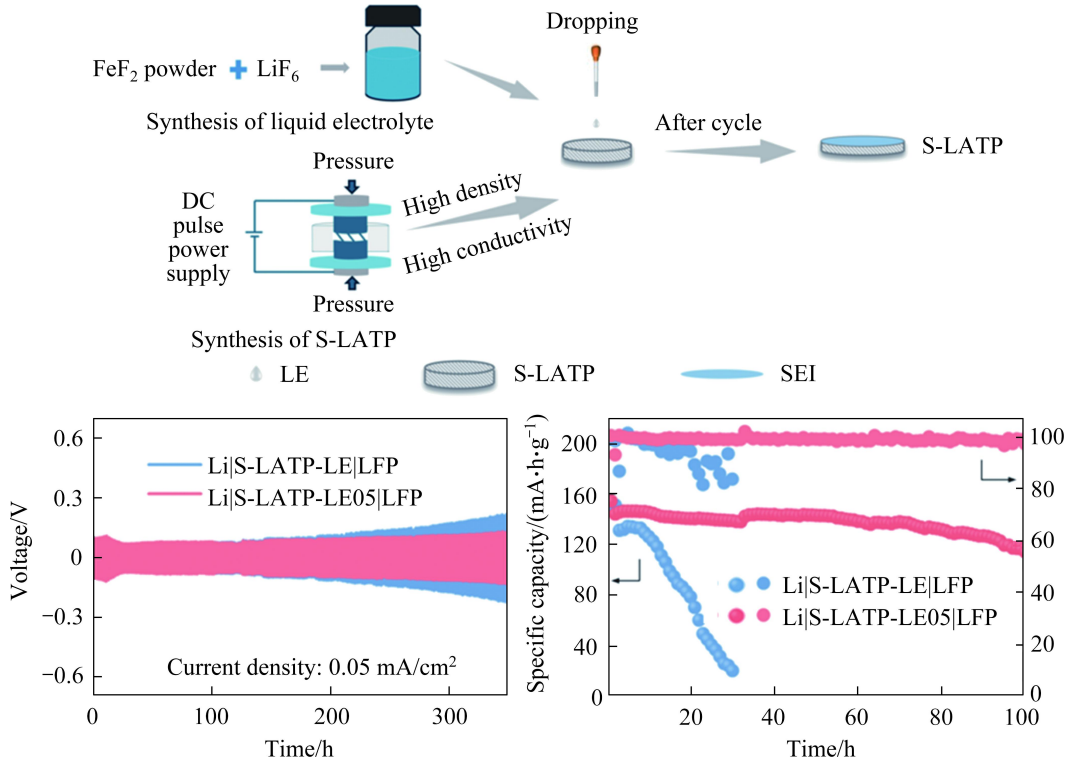


**Figure S1** Schematic diagram of S-LATP, the solid−liquid hybrid battery structure, and the morphology evolution process of S-LATP-LE05

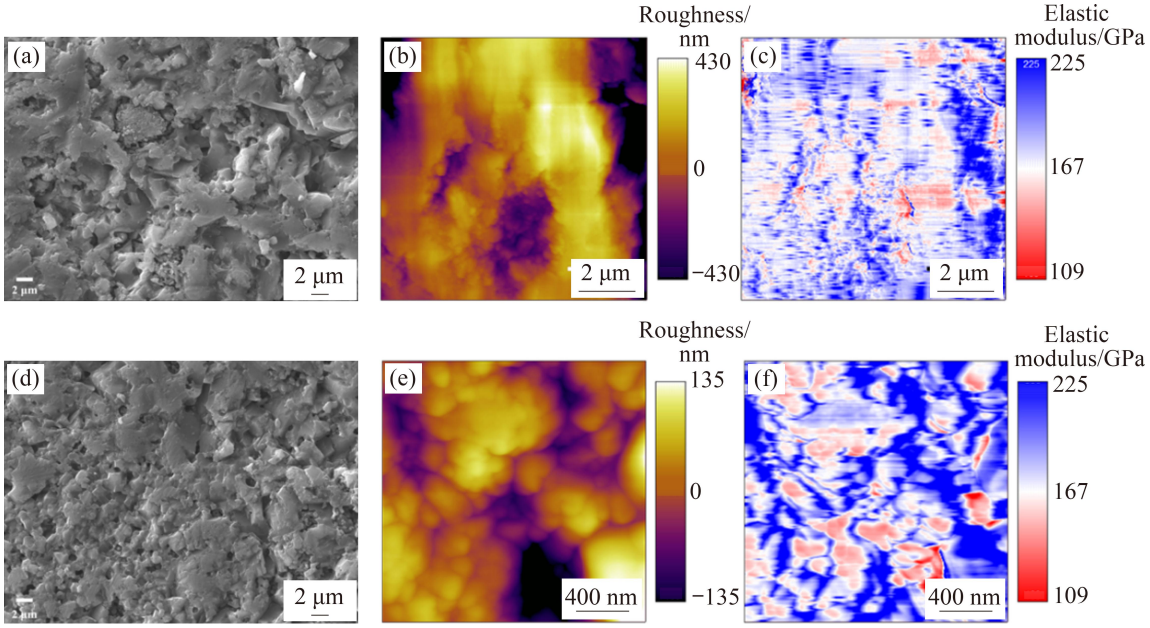


**Figure S2** The SEM images, the AFM morphology and elastic modulus of (a−c) 900 °C−30 MPa S-LATP and (d−f) 900 °C−40 MPa S-LATP

**Table S1** Density and relative density of LATP

| Condition (Sintering temperature (°C)-heating rate (°C/min)-pressure (MPa)) | Density/(g·cm$^{-3}$) | Relative density/% |
|---|---|---|
| 900-200-30 | 2.886 | 98.16 |
| 900-200-35 | 2.892 | 98.36 |
| 900-200-40 | 2.904 | 98.78 |
| C-LATP | 2.638 | 89.73 |

**Table S2** Ionic conductivity of LATP

| Condition (Sintering temperature (°C)-heating rate (°C/min)-pressure (MPa)) | Ionic conductivity/(S·cm$^{-1}$) |
|---|---|
| 900-200-30 | $5.06\times10^{-4}$ |
| 900-200-35 | $5.78\times10^{-4}$ |
| 900-200-40 | $4.94\times10^{-4}$ |
| C-LATP | $1.81\times10^{-4}$ |

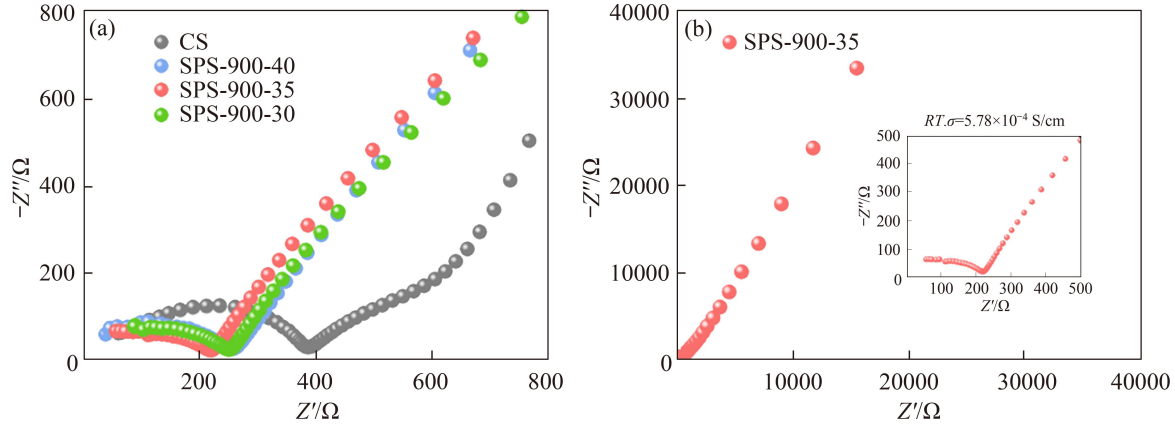


**Figure S3** The EIS test results: (a) 900 °C−30 MPa, 900 °C−35 MPa, 900 °C−40 MPa S-LATP and C-LATP; (b) 900 °C−35 MPa S-LATP (inset image is the corresponding ionic conductivity)

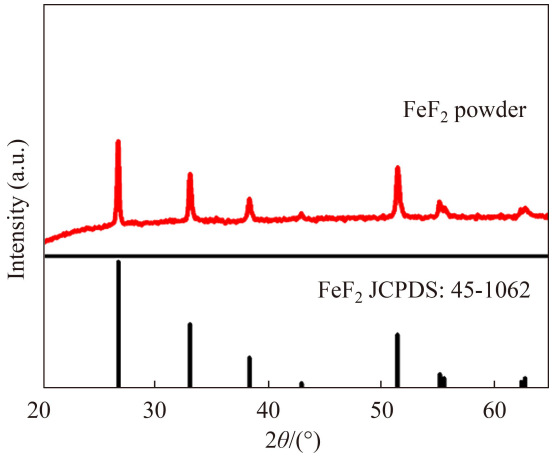


**Figure S4** The XRD test result of $FeF_2$ powder

**Table S3** Comparison of the cycling performance of the symmetric Li-Li cells

| Refs. | Type of LEs | Usage of LEs | Solid electrolyte | Performance |
|---|---|---|---|---|
| This work | 0.5 wt% $FeF_2$ LE | 4 μL/cm$^2$ | LATP | 0.05 mA/cm$^2$, 0.05 mA·h/cm$^2$, 350 h |
| [1] | 15 vol.% LE | — | LATP | 0.1 mA/cm$^2$, 0.05 mA·h/cm$^2$, 300 h |
| [2] | LiTFSI-$Pyr_{13}$FSI | 2.65 μL/cm$^2$ | LSPS | 0.115 mA/cm$^2$, 0.115 mA·h/cm$^2$, 350 h |
| [3] | 12% LE-CPE | — | LATP | 0.5 mA/cm$^2$, 0.25 mA·h/cm$^2$, 300 h |
| [4] | LiTFSI-$Pyr_{13}$TFSI | ~10 μL | LGPS | 0.038 mA/cm$^2$, 0.038 mA·h/cm$^2$, 1200 h |

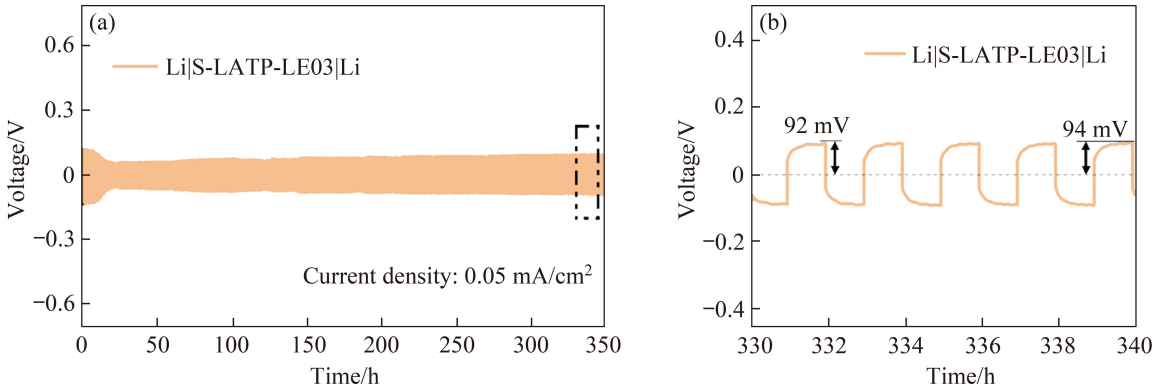


**Figure S5** (a) Voltage curve of Li|S-LATP-LE03|Li symmetric battery at 0.05 mA/cm$^2$; (b) Enlarged graph from 330 h to 340 h

**Table S4** Comparison of the cycling performance of the full battery

| Refs. | Types of LEs | Usage of LEs | Solid electrolyte | Cathode/Anode | Performance |
|---|---|---|---|---|---|
| This work | 0.5 wt% $FeF_2$ LE | 4 μL/cm$^2$ | LATP | LFP/Li | 78.1% after 100 cycles at 0.5*C* (1*C*=170 mA·h/g) |
| [1] | 15 vol.%LE | — | LATP | LFP/Li | 92.6% after 100 cycles at 0.5*C* (1*C*=170 mA·h/g) |
| [2] | LiTFSI-$Pyr_{14}$FSI | 2.65 μL/cm$^2$ | LLZO | LFP/Li | 45 cycles without decay at 20 mA/g |
| [3] | 12%LE-CPE | — | LATP | LFP/Li | 96% after 250 cycles at 0.1*C* (1*C*=170 mA·h/g) |
| [4] | LiTFSI-$Pyr_{13}$TFSI | ~10 μL | LGPS | S@C/Li | 82.6% after 50 cycles at 83.5 mA/g |
| [5] | LiTFSI/$Pyr_{13}$TFSI | 10 mg | LSPS | LFP/Li | 84.7% after 30 cycles at 14 mA/g |

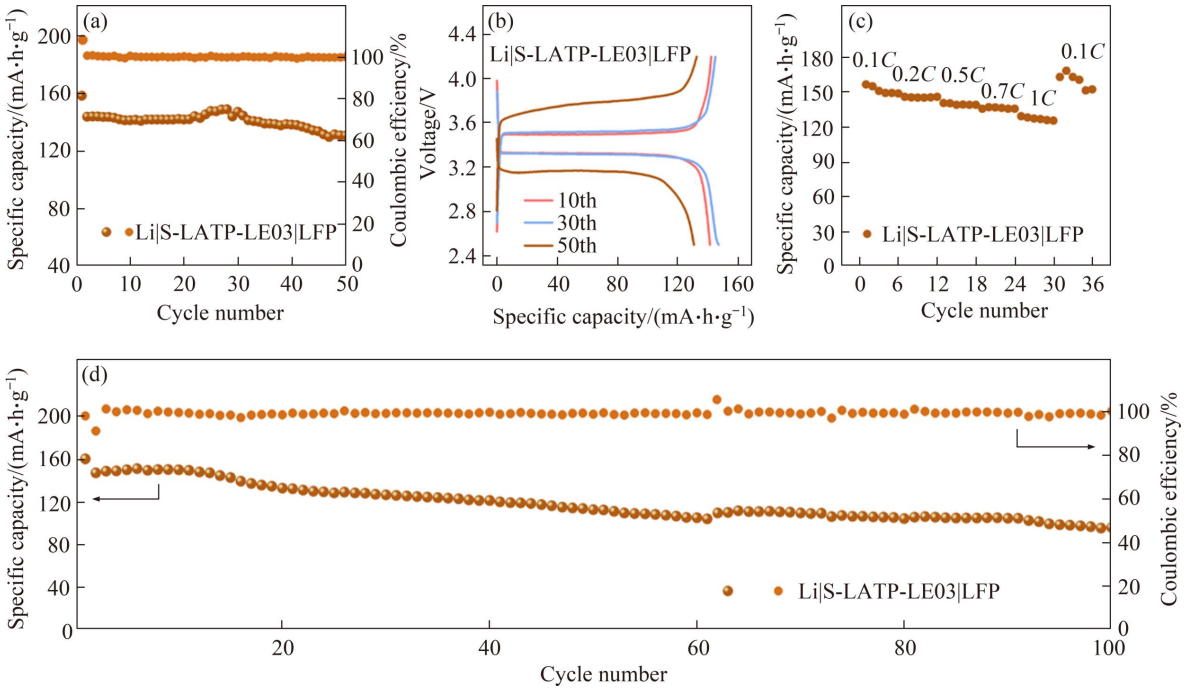


**Figure S6** Electrochemical performances of Li|S-LATP-LE03|$LiFePO_4$ full cell: (a) Cycling performance at 0.2*C*; (b) Selected voltage profiles at 0.2*C* (10, 30 and 50 cycles); (c) Rate performance; (d) Cycling performance at 0.5*C*

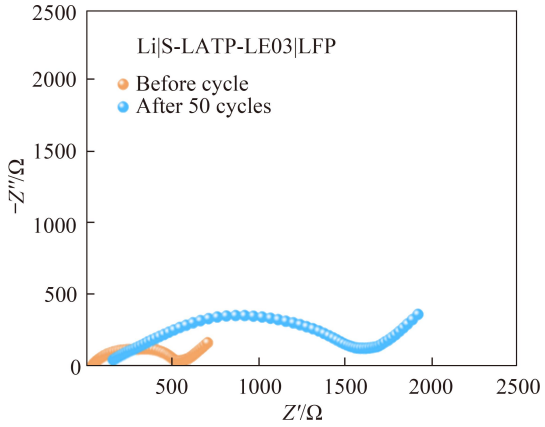


**Figure S7** EIS Nyquist plot of pristine Li|S-LATP-LE03|$LiFePO_4$ full cell and after 50 cycles

## References


[1] TANG Jian-tao, WANG L, YOU Long-zhen, et al. Effect of organic electrolyte on the performance of solid electrolyte for solid-liquid hybrid lithium batteries [J]. ACS Applied Materials & Interfaces, 2021, 13(2): 2685−2693. DOI: 10.1021/acsami.0c19671.

[2] PERVEZ S A, KIM G, VINAYAN B P, et al. Overcoming the interfacial limitations imposed by the solid-solid interface in solid-state batteries using ionic liquid-based interlayers [J]. Small, 2020, 16(14): e2000279. DOI: 10.1002/smll.202000279.

[3] TANG Jian-tao, WANG L, TIAN Chang-hao, et al. Double-protected layers with solid-liquid hybrid electrolytes for long-cycle-life lithium batteries [J]. ACS Applied Materials & Interfaces, 2022, 14(3): 4170−4178. DOI: 10.1021/acsami.1c21457.

[4] UMESHBABU E, ZHENG Bi-zhu, ZHU Jian-ping, et al. Stable cycling lithium-sulfur solid batteries with enhanced Li/$Li_{10}GeP_2S_{12}$ solid electrolyte interface stability [J]. ACS Applied Materials & Interfaces, 2019, 11(20): 18436−18447. DOI: 10.1021/acsami.9b03726.

[5] ZHENG Bi-zhu, ZHU Jian-ping, WANG Hong-chun, et al. Stabilizing $Li_{10}SnP_2S_{12}$/Li interface via an in situ formed solid electrolyte interphase layer [J]. ACS Applied Materials & Interfaces, 2018, 10(30): 25473−25482. DOI: 10.1021/acsami.8b08860.